

# **A COMPUTATIONAL AND EXPERIMENTAL STUDY OF THE INTERNAL FLOW IN A SCALED PRESSURE-SWIRL ATOMIZER**

**K. G. Hansen\*, J. Madsen\*\*, C. M. Trinh\*\*\*, C. H. Ibsen\*, T. Solberg\***  
**and B. H. Hjertager\***

granly@aue.auc.dk

**\* Chemical Engineering Laboratory, Aalborg University Esbjerg, Niels Bohrs Vej 8, DK-6700 Esbjerg, Denmark**

**\*\* FLS Miljø A/S, Ramsingvej 30, DK-2500 Valby, Denmark**

**\*\*\* Danfoss A/S, Nordborgvej 81, DK-6430 Nordborg, Denmark**

## **Abstract**

The internal flow in a scaled pressure-swirl atomizer has been studied both numerically and experimentally. The atomizer is a scale-up of a Danfoss pressure-swirl atomizer designed for domestic boilers. The atomizer is operated with water. The main objective of the work is to investigate whether it is possible to model the internal gas-liquid flow of an atomizer by use of the commercial code CFX-4.3. Special emphasis is given to the flow of the liquid phase. Laser Doppler Anemometry (LDA) measurements have been performed in the atomizer at a flow rate of 15 and 50 L/min respectively. Profiles of axial and tangential mean and RMS velocities are obtained. Furthermore, pressure measurements are conducted and pictures of the air-core and spray-cone are taken for qualitative comparison. The tangential velocity profile resembles a Rankine vortex as reported by [1] and [2]. Transient computational fluid dynamics, CFD, simulations have been performed in a three-dimensional curvilinear grid representing the swirl chamber of the atomizer. The gas-liquid flow is modelled with the homogeneous multi-phase model in CFX-4.3. Two approaches are used in the simulations: A Large Eddy Simulation, LES, based on the work of [3] and a simulation where the flow is modelled as being laminar. The simulations manage to capture the overall flow characteristics of a pressure-swirl atomizer with the formation of an air-core and a thin liquid film in the exit region of the swirl chamber. The numerical grid is able to resolve vortices in the liquid in the upper part of the swirl chamber. The trends in mean and RMS tangential velocity are captured, but the magnitude of the velocity is underestimated. With a modified inlet velocity in the laminar case, the magnitude of the tangential velocity shows better agreement with measurements demonstrating the importance of having representative inlet boundary conditions

## **Introduction**

Atomization is widely used in several applications, e.g. spray combustion, spray-painting, spray drying etc. Spray combustion is used in domestic heating burners, industrial furnaces, gas turbines, diesel engines and rockets. For combustion in domestic heating burners the pressure swirl or simplex atomizer has been found to be the cheapest and most reliable type of atomizer.

The internal flow characteristics in pressure-swirl atomizers are important, because they govern the thickness of the sheet formed at the discharge orifice. The internal flow also governs the magnitude of the axial, tangential and radial velocity components of the sheet and hence the break-up of the film and characteristics of the resulting spray.

The internal flow of pressure-swirl atomizers has been studied both numerically and experimentally e.g. [1], [2] and [4]. To the authors' knowledge only [1] and [2] have published LDA measurements inside an atomizer. Particle Image Velocimetry is used to visualize the air-core in [4].

Numerical studies of the internal flow have often been performed assuming axisymmetric flow. e.g. [1], [4], [5] and [6]. In [1] the flow is simplified to a single phase and the air-core diameter is not predicted. [4] predicts the air-core diameter with a free-surface routine, which adjusts the grid until the pressure at the boundary is equal to ambient pressure. But still only the flow of the liquid is computed. Conservation equations for both air and liquid are solved in [6], where the air-core is assumed to be entirely cylindrical. The diameter of the air-core is found from pressure-drop calculations, where it is found that the pressure-drop does not change with increasing diameter up to a critical value. Beyond this diameter, which is used in the calculations, the pressure drop increases with any increase in air-core diameter.

A three-dimensional multi-fluid simulation is presented in [7], where the cavitating flow inside an Diesel swirl injector is studied, the simulations give good qualitative results, but these are not validated against experimental results as done in [1] and [4].

In the present work a 3D numerical simulation will be performed using the commercial code CFX-4.3. The results from the simulations will be validated against experimental data obtained from LDA and pressure measurements inside an atomizer model.

### Experimental setup

The atomizer used in the measurements is a scale-up of a typical Danfoss nozzle. The atomizer is operated with water for practical reasons. An exchangeable cone is placed inside the atomizer. This cone forms the grooves that lead the water into the swirl chamber. The geometry of the swirl chamber is shown in Figure 1. A conical plexiglas tube forms the swirl chamber, which has a diameter,  $d_s$ , of 100 mm. The exit is cylindrical with a length,  $L_o$ , of 30 mm and a diameter,  $d_o$ , of 20 mm. The conical atomizer is placed inside a rectangular box, in order to minimize the change in direction of the laser beams due to differences in refractive indices. The atomizer is placed in the lid of a storage tank. The water is pumped from the tank through a flow meter. The pressure along the atomizer wall is monitored using pressure transmitters. The water is seeded with polyamide with a diameter of 50  $\mu\text{m}$  and a density of 1030  $\text{kg/m}^3$ .

The 2D Laser Doppler Anemometry setup used is from Dantec Dynamics A/S. The setup gives information about mean and RMS axial and tangential velocities. Due to differences in refractive indices only one velocity component could be obtained at a time.

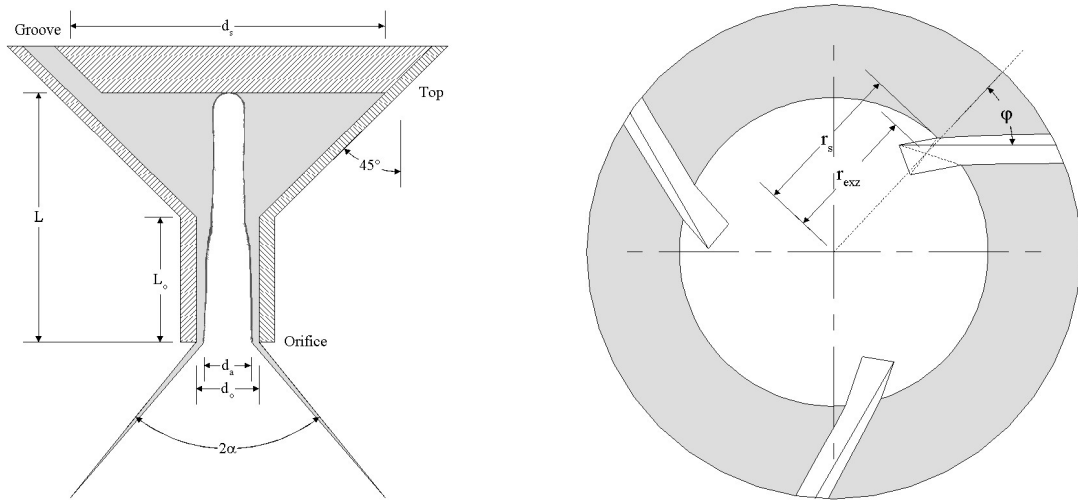


**Figure 1. Geometry of the swirl chamber (left) and the cone that forms the inlet grooves (right).**

With origin defined at the top of the swirl chamber at the centre axis the points of measurement are placed from -5 to -25 mm in axial and from -10 to -40 mm in radial direction, see Figure 2. The velocities are measured by randomizing the points of measurement and measuring 2 minutes in each point. This is done five times, and the results presented are averaged over the five measurements.

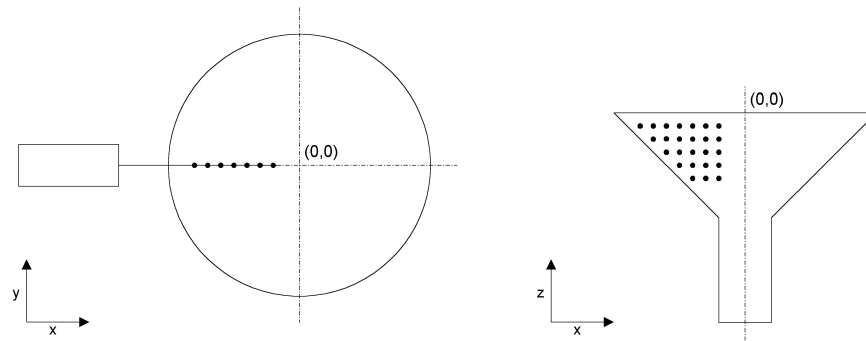


**Figure 2. Points of measurement inside the atomizer.**

### Numerical Simulations

Transient simulations are carried out with a three-dimensional representation of the swirl-chamber in the atomizer model. The homogenous multi-phase model in CFX-4.3 is used to predict the gas-liquid flow. The simulations performed are concentrated on two cases with a flow rate of 15 and 50 L/min respectively.

The homogeneous model assumes that a transported property,  $\Phi$ , for each phase are the same, [8]:

$$\Phi_m = \Phi, \quad 1 \leq m \leq N_p \quad (1)$$

Where the  $m$  and  $N_p$  are phase  $m$  and the total number of phases respectively. The governing equations written in tensor notation may be formulated as:

Mass balance:

$$\frac{\partial}{\partial t} \rho + \frac{\partial}{\partial x_i} \rho U_i = 0 \quad (2)$$

Where  $\rho$  and  $U$  are the density and velocity respectively.

Momentum equation:

$$\frac{\partial}{\partial} (\rho U_i) + \frac{\partial}{\partial x_j} (\rho U_i U_j) = \frac{\partial}{\partial x_j} \left( \mu_{eff} \left[ \frac{\partial U_j}{\partial x_i} + \frac{\partial U_i}{\partial x_j} \right] \right) + B_i - \frac{\partial P}{\partial x_i} \quad (3)$$

Where  $\mu_{eff}$ ,  $B$  and  $P$  are the effective viscosity, the body forces and pressure respectively. The effective density,  $\rho$ , and viscosity are given by:

$$\rho = \sum_{m=1}^{N_p} \alpha_m \rho_m \quad (4)$$

$$\mu_{eff} = \sum_{m=1}^{N_p} \alpha_m \mu_{m,eff} \quad (5)$$

Where  $\alpha_m$  and  $\mu_{m,eff}$  is the volume fraction and effective viscosity of phase  $m$  respectively.

Two modelling strategies are followed: one where the flow is treated as being laminar and a Large Eddy Simulation (LES). In the first case the effective viscosity is equal to the laminar or molecular viscosity. In LES the effective viscosity is a sum of the laminar viscosity and a sub-grid scale (SGS) viscosity,  $\mu_{m,SGS}$ :

$$\mu_{m,eff} = \mu_{m,lam} + \mu_{m,SGS} \quad (6)$$

The SGS viscosity is found from an eddy-viscosity hypothesis first used by Smagorinsky [9]:

$$\mu_{m,SGS} = \rho (C_s \Delta)^2 (\bar{S}_{ij} \bar{S}_{ij})^2 \quad (7)$$

Where  $C_s$ ,  $\Delta$ , and  $S_{ij}$  are an eddy viscosity constant, the filter length scale and the strain rate tensor for the resolved field respectively. The implementation in CFX-4.3 is based on [3].

When using the homogeneous model to calculate gas-liquid flow with a free surface between the phases, a surface-sharpening algorithm is available in CFX-4.3. When calculating the two-phase flow, it is possible that the interface becomes smeared out, owing to numerical diffusion in the void fraction. The algorithm defines the surface as being where the volume fraction is equal to 0.5. The code then identifies fluid on the wrong side of the interface and moves it to the correct side of the interface ensuring that volume is conserved [8].

### Numerical settings

In order to capture the flow characteristics in the atomizer a three-dimensional calculation domain is chosen. In the present work special emphasis is given to the internal flow in the swirl-chamber, so only this part of the atomizer is modelled. The inlet velocity forms a flat profile that follows the direction of the inlet grooves.

During some preliminary test-runs it was found that it is necessary to have a high grid resolution around the air-core in order to maintain the air-core inside the swirl chamber. In order to maintain a high resolution the geometry is divided into a 9-block structure. The block structure and the resulting grid may be seen in Figure 3. The grid consists of 95,697 cells.

For the simulations the time-step is determined from a Courant number at the orifice of the atomizer based on the axial velocity of the water. This gives a time-step of  $4.0 \times 10^{-4}$  s in the case with a flow rate of 15 L/min and a time-step of  $1.25 \times 10^{-4}$  s in the case with a flow rate of 50 L/min.

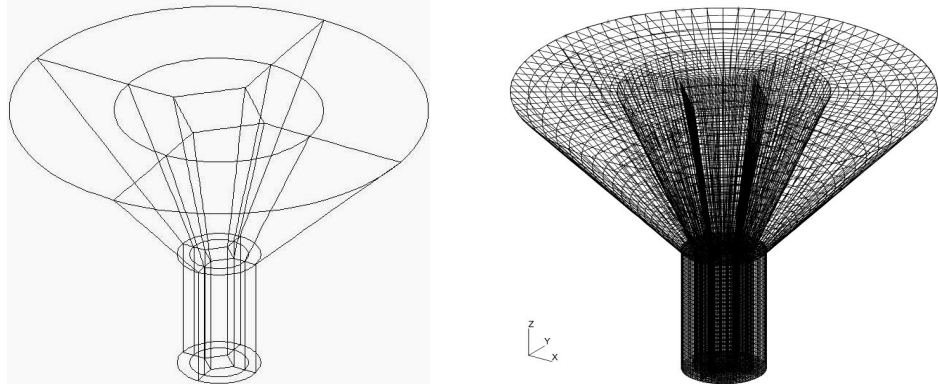


**Figure 3. The block structure of the calculation domain (left) and the resulting grid (right).**

## Results

The simulations are run between 0.6 and 2.5 seconds of real time, depending on the size of the time-step. The results are averaged over the last 4000 time-steps and compared to experimental results. The trend for the simulations is similar both when the flow rate and/or the turbulence modelling are changed.

Initially the atomizer is gradually filled with water until an air-core similar to the one seen in the experiments is formed. After the initial filling of the atomizer the flow approaches a "quasi steady state", with periodic fluctuations and oscillations. In Figure 4 an instantaneous flow field is shown. The air-core is represented by a surface corresponding to a volume fraction of 0.5. In the upper left part of the swirl chamber vortices are formed and are moving downwards along the wall of the atomizer. [4] reported similar structures in the flow field inside various atomizers from axisymmetric simulations.

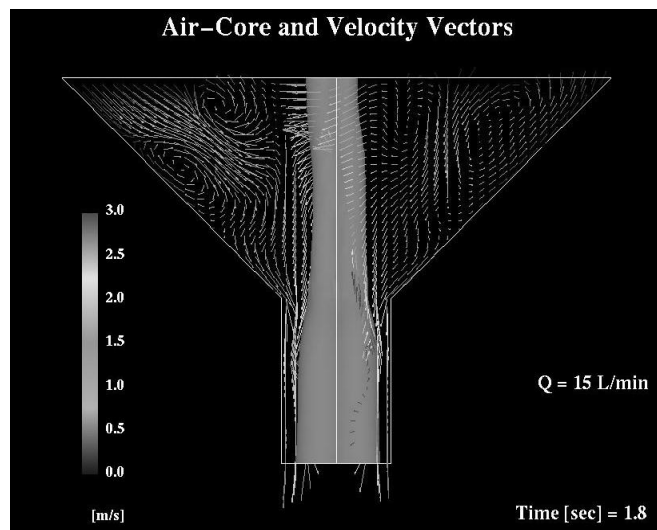


**Figure 4. Air-core and velocity vectors after 1.8 seconds of simulations at a flow rate of 15 L/min. The vectors are normalized.**

The measured tangential velocity as a function of radial position is almost constant at all axial positions and resembles a Rankine vortex as reported by [1] and [2].

Figure 5 shows the mean tangential and axial velocity from simulations compared with LDA measurements at an axial position of -10 mm at a flow rate of 50 L/min. The simulations and the experiments show similar trends in the tangential velocity, but the velocity is under-estimated by the simulations. The velocities from the laminar simulations are under-estimated by a factor of two and the velocities from LES are even lower. In order to test the influence of the inlet velocity profile a laminar simulation with a modified inlet velocity is performed. An estimate for the tangential and radial velocities at the inlet are found by multiplying the velocities found

from the inlet grooves by a factor of 2, but maintaining the flow rate. This approach gives better agreement between simulated and measured velocities.

The magnitude of axial velocities predicted from laminar simulations are in agreement with measurements, but the trend in axial velocity as a function of radius does not follow the measurements. The simulated axial velocities show the same general trend as the measured ones, however the magnitude and position of the local extrema differ somewhat.

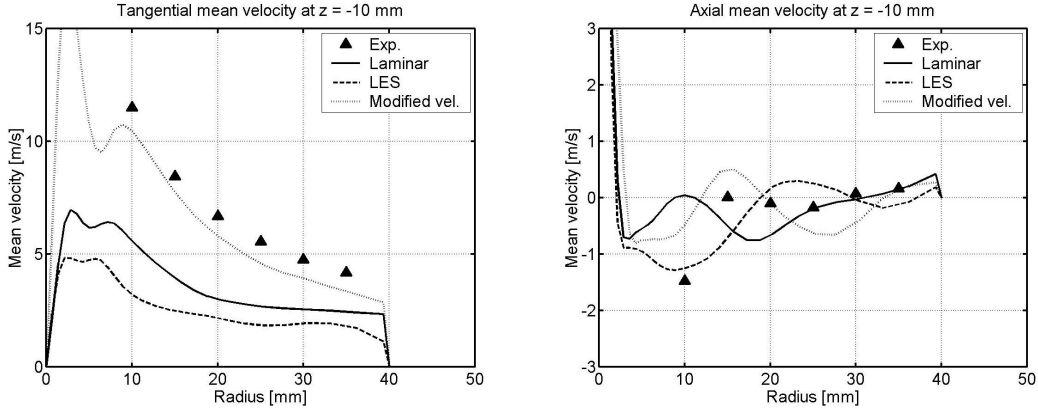


**Figure 5. Comparison of mean tangential (left) and axial (right) velocities at z= -10 mm from Simulations and experiments at a flow rate of 50 L/min.**

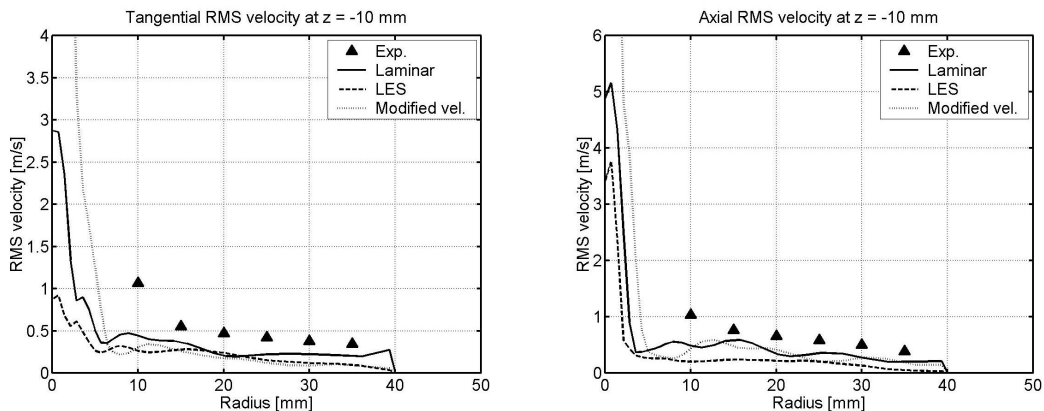


**Figure 6. Comparison of tangential RMS (left) and axial RMS (right) velocities at z= -10 mm from Simulations and experiments at a flow rate of 50 L/min.**

Comparisons of tangential and axial RMS velocities obtained from simulations and LDA measurements are shown in Figure 6. The simulations capture the general trend with a flat profile at a higher radius and an increase at a lower radius. The RMS velocity obtained from simulations is generally lower than RMS values obtained from LDA measurements. Due to the increase in viscosity predicted by LES the RMS values are lower than the ones predicted by the laminar simulations. RMS values from LES are lower than the ones predicted by the laminar simulations. This arises from the increase in viscosity predicted by LES, which dampens the oscillations in the flow. The discrepancy near the air-core where the simulations fail to predict the sudden increase in RMS is either a consequence of the measurements being biased by the air-core or that the simulation are unable to capture fluctuations in the near-core region.

Comparisons of pressure at the wall of the atomizer obtained from simulations and measurements are seen in Figure 7. The discontinuities in the calculated pressure profiles arise from the change in the geometry from a conical to cylindrical shape. The laminar simulation and the simulation using LES underestimate the pressure, whereas the simulation with modified velocity overestimates the pressure. The difference in pressure between the simulations arises from the difference in tangential velocity. This can be expressed as:

$$P \sim u_t^2 \quad (8)$$

The discrepancies in velocities and pressure may be encountered by modelling the flow in the inlet grooves and thereby obtain a more representative velocity profile at the inlets.

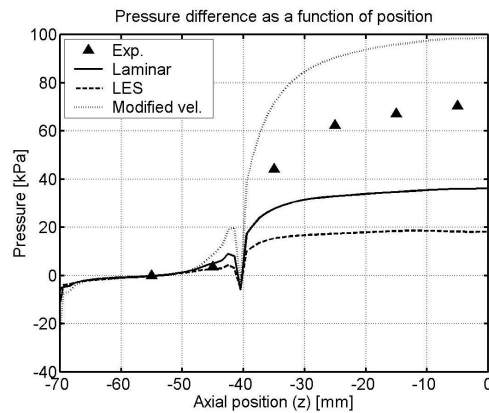


**Figure 7. Comparison of pressure at the wall from experiments and simulations. The values are calculated as the difference between the absolute pressure and the pressure at  $z = -55$  mm at a flow rate 50 L/min.**

## Conclusions

The internal flow in a scaled pressure-swirl atomizer has been studied both numerically and experimentally. The numerical results have been verified against results from LDA measurements and pressure measurements.

The trends obtained in the measurements agree with the ones reported in [1] and [2]. The tangential velocity profile resembles a Rankine vortex.

Simulations assuming laminar flow and Large Eddy Simulations are able to predict the overall flow conditions in the atomizer. An air-core is maintained throughout the time of simulation. The grid is able to resolve vortices in the liquid in the upper part of the swirl chamber. The trends in mean and RMS tangential velocity are captured, but the magnitude of the velocity is underestimated. With a modified inlet velocity in the laminar case, the magnitude of the tangential velocity shows better agreement with measurements demonstrating the importance of having representative inlet boundary conditions. The simulated axial velocities show the same general trend as the measured ones. However the magnitude and position of the local extrema differ somewhat. The axial RMS velocity from simulations is underestimated in the upper part of the swirl chamber, but shows better agreement at lower axial positions.

## References

- [1] Horvay, M., *Theoretische und experimentelle Untersuchung über den Einfluss des inneren Strömungsfeldes auf die Zerstäubungseigenschaften von Drall-Druckzerstäubungsdüsen*, PhD.-thesis, Universität Karlsruhe, 1985, p. 121.
- [2] Löffler-Mang, M., and Leuckel, W., "Atomization with Spill-Controlled Swirl Pressure-Jet Nozzles", *ICLASS-91*, Gaithersburg, MD, USA, July 1991, pp. 431-440.
- [3] Jacobsen C. B., *Large Eddy Simulation of Confined Swirling Flow – Numerical Part*, PhD.-thesis, Aalborg University, 1997, p. 171.
- [4] Yule, A.J., and Chinn, J.J., "The Internal Flow and Exit Conditions of Pressure Swirl Atomizers", *Atomization and Sprays*. 10, 121-146, (2000).
- [5] Nonnenmacher, S. and Piesche, M., "Design of Hollow Cone Pressure Swirl Nozzles to atomize Newtonian Fluids", *Chem. Eng. Sci.* 55, 4339-4348, (2000).
- [6] Datta, A., and Som, S.K., "Numerical Prediction of Air Core Diameter, Coefficient of Discharge and Spray Cone Angle of a Swirl Spray Pressure Nozzle", *Int. J. Heat and Fluid Flow*. 21, 412-419, (2000).
- [7] Alajbegovic, A., Meister, G., Greif, D., and Basara, B., "Three Phase Cavitating Flows in High Pressure Swirl Injectors", *Fourth International Conference on Multiphase Flow*, New Orleans, Louisiana, USA, May-June 2001, pp. 1-7.
- [8] AEA Technology plc. *CFX-4.3 Solver*, AEA Technology plc., 1997.
- [9] Smagorinsky, J., "General Circulation Experiments with the Primitive Equations, Part I: The Basic Experiment". *Monthly Weather Rev.* 91, 99-164, (1963).